ELSEVIER

Biochemical Pharmacology 62 (2001) 1409–1415

Biochemical Pharmacology

Blood-brain barrier and neuronal membrane transport of 6-[^{18}F]fluoro-L-DOPA

Randa E. Yee, David W. Cheng, Sung-Cheng Huang, Mohammad Namavari, Nagichettiar Satyamurthy, Jorge R. Barrio*

Department of Molecular and Medical Pharmacology, UCLA School of Medicine, B2-086A Center of the Health Sciences, Los Angeles, CA 90095-6948, USA

Received 23 January 2001; accepted 18 April 2001

Abstract

The transport of 6-[^{18}F]fluoro-L-3,4-dihydroxyphenylalanine ([^{18}F]FDOPA) across the blood-brain barrier (BBB) and neuronal membranes was compared with that of L-3,4-dihydroxyphenylalanine (L-DOPA) in rats. The carotid injection method was used as a direct measurement of [^{18}F]FDOPA, 1-[^{14}C]-L-DOPA, and 3-[^{14}C]-L-DOPA transport across the BBB, while isolated nerve terminals were used to examine neuronal membrane transport of [^{3}H]-L-DOPA. [^{18}F]FDOPA appeared to use the same large neutral amino acid carrier for BBB transport as L-DOPA and L-phenylalanine. In addition, carbidopa [L-α-hydrazino-α-methyl-β-(3,4-dihydroxyphenyl)propionic acid] was found not to have direct interference with the transport carrier on the BBB, but indirectly inhibited aromatic L-amino acid decarboxylase (AAAD) activity in brain endothelium by depletion of pyridoxal phosphate, a necessary cofactor of the enzyme. In striatal and cortical synaptosomes, [^{3}H]-L-DOPA uptake was inhibited by non-radioactive L-DOPA, FDOPA, and 6-fluoro-L-*meta*-tyrosine (6-FMT). The inhibition was significantly greater in terminals isolated from the striatum than in those from the cerebral cortex. FDOPA, 6-FMT, and L-DOPA equally inhibited the neuronal transport of [^{3}H]-L-DOPA. This suggests that FDOPA and 6-FMT compete with L-DOPA at similar transport sites at the neuronal membrane.

Keywords: AAAD; Brain uptake index; L-DOPA; Carbidopa; Synaptosomes

1. Introduction

[^{18}F]FDOPA was the first *in-vivo* "marker" of central dopamine synthesis [1,2]. Other presynaptic dopaminergic probes, such as 4-[^{18}F]FMT [3] and 6-[^{18}F]FMT [4], dopamine reuptake ligands [5], and dopamine vesicle probes [6] soon followed. However, [^{18}F]FDOPA remains an important clinical marker for PD, and is indicated for the evaluation of functional activity within dopaminergic systems in humans. The administration of [^{18}F]FDOPA leads to the accumulation of tracer in striatal tissue, a region rich in dopaminergic neurons, when the system is intact and functional. That accumulation does not occur, however, when the functional integrity of the dopamine system is compromised (e.g. PD or MPTP-induced parkinsonism) [7–9]. Therefore, [^{18}F]FDOPA has been used to evaluate the integrity of presynaptic dopaminergic mechanisms within the CNS.

The enhancement of our understanding of PET measurements and, in turn, the development of more reliable techniques for analyzing and interpreting results from [^{18}F]FDOPA studies will be dependent upon a well-characterized model for the kinetics of [^{18}F]FDOPA. The ability to quantitate data derived from PET will allow for the detection of comparative changes in dopaminergic systems *in-vivo*. However, quantitation of [^{18}F]FDOPA-PET kinetic data to extrapolate rate constants depends upon knowledge of the biological system being examined [10].

* Corresponding author. Tel.: +1-310-825-4167; fax: +1-310-825-4517.

E-mail address: jbarrio@mednet.ucla.edu (J.R. Barrio).

Abbreviations: AAAD, aromatic L-amino acid decarboxylase; BBB, blood-brain barrier; BUI, brain uptake index; carbidopa, L-α-hydrazino-α-methyl-β-(3,4-dihydroxyphenyl)propionic acid; L-DOPA, L-3,4-dihydroxyphenylalanine; FDA, 6-fluorodopamine; [^{18}F]FDOPA, 6-[^{18}F]fluoro-L-3,4-dihydroxyphenylalanine; 4-[^{18}F]FMT, 4-[^{18}F]fluoro-L-*meta*-tyrosine; 6-[^{18}F]FMT, 6-[^{18}F]fluoro-L-*meta*-tyrosine; MeAIB, α-(methylamino) isobutyric acid; MPTP, 1-methyl-1,2,3,6-tetrahydropyridine; PD, Parkinson's disease; PET, positron emission tomography; and PLP, pyridoxal phosphate.

0006-2952/01/$ – see front matter
PII: S0006-2952(01)00787-0

The specific accumulation of [^{18}F]FDOPA within the basal ganglia is presumed to follow a pathway of transport and metabolism similar to that of L-DOPA. Previous investigations demonstrated that *in vivo* metabolism of [^{18}F]FDOPA, both in the CNS and peripherally, does parallel that of L-DOPA [11–13]. Indeed, the central metabolic behavior of [^{18}F]FDOPA coincides with that of the endogenous dopamine system in all cases evaluated (e.g. pharmacological modulation and electrical stimulation) [14–16]. Centrally, [^{18}F]FDOPA is decarboxylated to [^{18}F]FDA, which is stored in vesicles, released, and then broken down to metabolites [11]. It was assumed earlier that [^{18}F]FDOPA crosses the BBB via the same transport mechanism as L-DOPA, namely the L-system large neutral amino acid (LNAA) carrier [17]. Likewise, the presence of an L-system transporter on the surface of striatal neurons [18] suggests that [^{18}F]FDOPA may also enter dopamine neurons by a similar mechanism. However, it has not been assessed whether the transport of [^{18}F]FDOPA corresponds with that of L-DOPA at the BBB and neural plasma membranes.

In addition to membrane barriers, at which substrates entering are controlled by transport systems, enzymatic barriers can further restrict the entry of substances into the brain [19,20]. For example, brain capillary and peripheral tissue AAAD (EC 4.1.1.28) may play a major role in controlling the influx of L-DOPA into the brain. In PD patients, for example, the bioavailability of exogenous L-DOPA can be enhanced by the administration of carbidopa [21], thereby suppressing AAAD activity in peripheral tissues and cerebral microvessels [20]. Similarly, carbidopa is administered routinely in [^{18}F]FDOPA-PET determinations to enhance signal intensity in the striatum by suppressing peripheral [^{18}F]FDOPA decarboxylation [22,23]. Although PET kinetics have demonstrated that carbidopa did not affect the influx rate constant for [^{18}F]FDOPA from plasma to brain tissue [23], direct evidence on the effect of carbidopa on transport has not been obtained yet.

In this work we characterized the transport mechanism of [^{18}F]FDOPA in comparison to that of L-DOPA at the BBB and neuronal membranes. In addition, the effect of carbidopa on BBB transport of L-DOPA was also examined.

2. Materials and methods

2.1. Materials

1-[^{14}C]-L-DOPA (10.3 mCi/mmol) and 3-[^{14}C]-L-DOPA (15 mCi/mmol) were purchased from the Amersham Corp., while [^{3}H]H_2O was from DuPont-NEN. [^{3}H]-L-DOPA (60 Ci/mmol) was purchased from Moravek Biochemicals Inc. [^{18}F]FDOPA (2–5 Ci/mmol) and non-radioactive FDOPA and 6-FMT were synthesized as described previously [24, 25]. The purity of all radiolabeled products was always assessed immediately before experiments were performed. Triton X-100, liquid scintillation fluid, and micro protein determination kits were obtained from the Sigma Chemical Co. Soluene-350 tissue solubilizer was from Packard Instruments.

2.2. BUI measurements by carotid injections

All procedures were approved by the Animal Research Committee of the University of California at Los Angeles. Carotid injections were performed on male Sprague-Dawley rats (225–235 g) using the Oldendorf method [26], which directly quantitates the uptake of any compound of interest relative to the uptake of a reference compound (i.e. water). Where applicable, animals were pretreated subcutaneously with carbidopa (5 mg/kg) 60 min prior to carotid injection. After anesthesia with 150 mg/kg of ketamine and 1.5 mg/kg of xylazine, the common carotid was exposed and injected with a 0.2-mL bolus of either 0.083 μCi of 1-[^{14}C]-L-DOPA/0.042 μCi [^{3}H]H_2O or 0.121 μCi of 3-[^{14}C]-L-DOPA/0.605 μCi [^{3}H]H_2O in Ringer solution [10 mM HEPES (pH 7.4), 141 mM NaCl, 4 mM KCl, and 2.8 mM $CaCl_2$] with or without 270 μM PLP. For [^{18}F]FDOPA measurements, 0.667 μCi of [^{18}F]FDOPA/0.042 μCi [^{3}H]-H_2O was injected in Ringer solution alone, or containing 2 mM MeAIB, 0.5 mM L-phenylalanine, or 0.5 mM L-DOPA. After injections, syringes were rinsed with Ringer solution into a clean vial, counted, and [^{14}C]/[^{3}H] or [^{18}F]/[^{3}H] mixture ratios were determined. The animals were decapitated 15 sec after the bolus injection. Subsequently, the ipsilateral cerebral hemispheres were removed, extruded through a 20-gauge needle into two 20-mL glass scintillation vials, and incubated in 2 mL of Soluene-350 at 60° for 2 h. Samples were counted on a Packard 1900 CA Tricarb LS Analyzer for 20 min, after the addition of 10 mL of liquid scintillation fluid. Two protocols were programmed for counting. In one protocol, ^{3}H was counted in window A (0–12 keV) and ^{14}C was counted in window B (12–156 keV). In the other protocol, ^{3}H was counted in window A (0–12 keV) and ^{18}F was counted in window B (18.6–640 keV). In the case of [^{18}F]FDOPA samples, the vials were counted immediately, while ^{3}H signals were only counted 2 days later, after all the ^{18}F radionuclide (half-life: 109 min) had decayed away. Each experiment was repeated at least three times using different animals (data represents the average ± SD). The BUI was calculated as follows:

$$\mathrm{BUI} = \frac{\text{tissue} - {}^{14}\text{C (or } {}^{18}\text{F)/tissue} - {}^{3}\text{H}}{\text{mixture} - {}^{14}\text{C (or } {}^{18}\text{F)/mixture} - {}^{3}\text{H}} \times 100$$

One-way ANOVA was performed to assess if a significant difference ($P < 0.05$) was observed between the different treatment groups.

2.3. Transport measurements in isolated nerve terminals from rat brain

Synaptosomes were purified from striatum and cerebral cortex of Sprague-Dawley rat brains (to be described elsewhere). After isolation, the purified synaptosomes were resuspended in modified Krebs-Ringer medium [121.9 mM NaCl, 0.87 mM $CaCl_2$, 4.89 mM KCl, 1.23 mM $MgSO_4$, 10 mM sodium phosphate buffer (pH 7.4), 30 mM glucose, 2 mM ascorbic acid, and 1 mM EDTA]. Synaptosomes were aliquoted into culture tubes, and the tubes were preincubated in a waterbath at 37° for 10 min. Determination of transport across synaptosomal membranes was initiated by the simultaneous addition of [^{3}H]-L-DOPA to a final concentration of 25 nM and non-radioactive FDOPA, or 6-FMT. The final concentration of unlabeled substrates ranged from 0 to 50 μM in each culture tube containing approximately 0.1 mg of synaptosomal protein. Protein concentration was determined using a micro protein kit. The reaction was incubated in a waterbath at 37° for an additional minute, before the reaction was terminated by quenching with ice-cold Krebs-Ringer medium. Samples were filtered rapidly through a Whatman glass fiber filter (GF/C, 25 mm) attached to a vacuum manifold. The filter was washed three times with 4 mL of ice-cold Krebs-Ringer medium, and then transferred to a glass scintillation vial. Radioactivity was released from synaptosomal vesicles by overnight incubation with 1 mL of 1% Triton X-100. After the addition of 10 mL of liquid scintillation fluid, the samples were counted using a Packard 1900 CA Tricarb LS Analyzer.

Transport measurements were carried out in triplicate at least three times using different membrane preparations. Data represent the average ± SD, where the data are expressed in units of picomoles per minute per milligram of synaptosomal protein (pmol/min/mg). To compare the effects of unlabeled FDOPA, 6-FMT, and L-DOPA on [^{3}H]-L-DOPA neuronal transport, the relative rate of transport was calculated as follows:

$$\text{Relative rate} = \frac{\text{transport rate of [}^3\text{H]-L-DOPA in the presence of unlabeled substrate}}{\text{transport rate of [}^3\text{H]-L-DOPA in medium alone}}$$

One-way ANOVA was performed to assess if there was a significant difference ($P < 0.05$) in [^{3}H]-L-DOPA transport between the different brain regions, and between the relative rates of [^{3}H]-L-DOPA transport in the presence of FDOPA, 6-FMT, or L-DOPA.

3. Results

3.1. BBB transport

The BUIs for [^{18}F]FDOPA, 3-[^{14}C]-L-DOPA, or 1-[^{14}C]-L-DOPA under various conditions are shown in Table 1. [^{18}F]FDOPA and 3-[^{14}C]-L-DOPA produced comparable uncompeted BUIs of 30.7 ± 3.4 and 30.6 ± 3.6. In addition, when both compounds were coinjected into the common carotid artery, an [^{18}F]FDOPA/3-[^{14}C]-L-DOPA uptake ratio of near unity (1.05 ± 0.07) was observed. MeAIB did not interfere with [^{18}F]FDOPA BBB transport at a concentration of 2 mM. However, 0.5 mM L-phenylalanine and L-DOPA significantly inhibited [^{18}F]FDOPA BBB transport by 62% ($P < 0.005$) and 65% ($P < 0.001$), respectively. Pretreatment of animals with carbidopa resulted in a significant increase ($P < 0.0014$) in 1-[^{14}C]-L-DOPA BUI from 11.2 ± 2.6 to 21.7 ± 1.6, while the addition of 270 μM PLP restored the BUI of 1-[^{14}C]-L-DOPA to 12.5 ± 0.8. Carbidopa pretreatment did not alter the BUI of 3-[^{14}C]-L-DOPA, which was approximately three times greater than that of 1-[^{14}C]-L-DOPA. When 3-[^{14}C]-L-DOPA and 1-[^{14}C]-L-DOPA were coinjected with 0.3 or 3.0 μg/mL of carbidopa into the cartoid artery, the BUIs of both radiolabeled probes remained unchanged.

3.2. Neuronal membrane transport in rat brain

Analogs of L-DOPA and L-*meta*-tyrosine reduced the uptake of [^{3}H]-L-DOPA into striatal and cortical synaptosomes (Fig. 1), similar to findings observed with unlabeled L-DOPA (unpublished observation). The rate of [^{3}H]-L-DOPA transport across the neural plasma membrane decreased in the presence of increasing concentrations of FDOPA for both synaptosomal preparations. FDOPA reduced the relative rate of [^{3}H]-L-DOPA uptake by a maximum of 69 and 49% in striatal and cortical synaptosomes,

Table 1
Brain uptake indices (BUIs) of L-DOPA and FDOPA in rats

Substrate/Condition	BUI
L-3-[^{14}C]DOPA	30.6 ± 3.6
co-injected with 0.3 μg/mL carbidopa	28.0 ± 2.2
co-injected with 3.0 μg/mL carbidopa	29.7 ± 0.9
with 60 min carbidopa pretreatment	26.8 ± 1.7
L-1-[^{14}C]DOPA	11.2 ± 2.6*
co-injected with 0.3 μg/mL carbidopa	12.9 ± 0.6
co-injected with 3.0 μg/mL carbidopa	11.8 ± 2.8
with 60 min carbidopa pretreatment	21.7 ± 1.6
with 60 min carbidopa pretreatment and coinjection with 270 μM PLP	12.5 ± 0.8*
[^{18}F]FDOPA	30.7 ± 3.4
in 2 mM MeAIB	27.3 ± 1.3
in 0.5 mM L-phenylalanine	11.6 ± 4.9**
in 0.5 mM L-DOPA	10.7 ± 2.1**
[^{18}F]FDOPA/L-3-[^{14}C]DOPA	1.05 ± 0.07

BUIs were determined in rats by carotid injections of 1-[^{14}C]L-DOPA, 3-[^{14}C]L-DOPA, or 6-[^{18}F]fluoro-L-DOPA. [^{3}H]H_2O was used as an internal standard for all measurements. Data represent the average ($N = 3$) ± SD.

* Significant difference in the BUI of 1-[^{14}C]L-DOPA with $P < 0.001$) and without ($P < 0.004$) carbidopa and PLP pretreatment compared with the BUI of 1-[^{14}C]L-DOPA with carbidopa pretreatment only.

** Significant difference in the BUI of 6-[^{18}F]fluoro-L-DOPA in the presence of 0.5 mM phenylalanine $P < 0.005$) and 0.5 mM L-DOPA ($P < 0.001$).

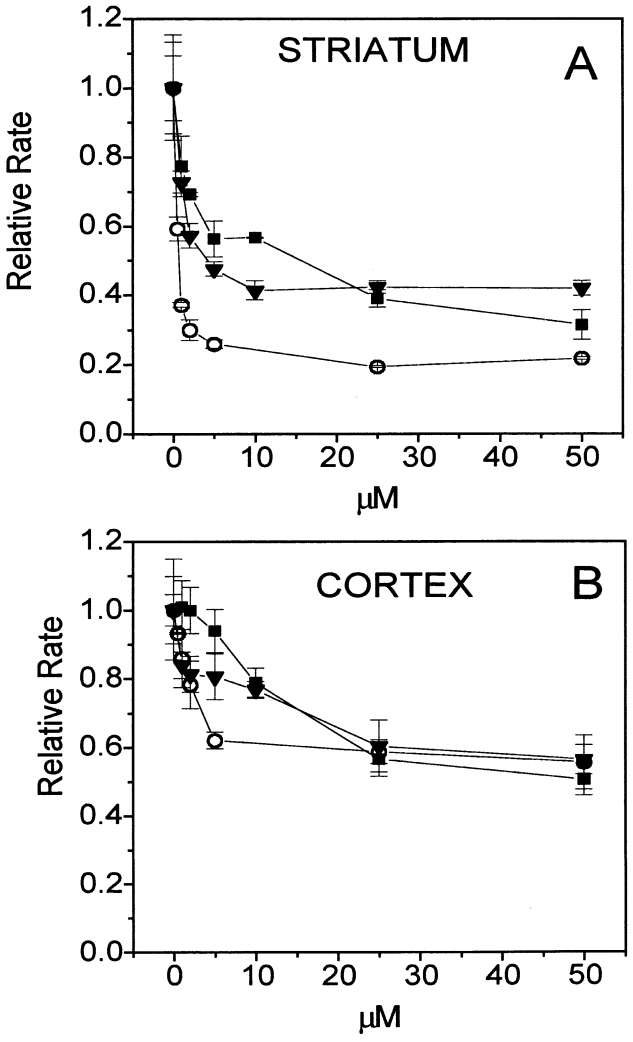

Fig. 1. Brain regional transport of [^{3}H]-L-DOPA in the presence of FDOPA, 6-FMT, and L-DOPA into rat brain synaptosomes. The effect of [^{3}H]-L-DOPA uptake by non-radioactive FDOPA (■), 6-FMT (▼), and L-DOPA (○) was measured in isolated synaptosomes from rat striatum (A) and cerebral cortex (B). Synaptosomes were preincubated in modified Krebs-Ringer medium at 37° for 10 min. Subsequently, synaptosomes were incubated for an additional minute in 25 nM [^{3}H]-L-DOPA and either 0, 0.5 (or 1), 2, 5, 10, 25, or 50 μM FDOPA, 6-FMT, or L-DOPA. Data represent the average ± SD (N = 3). One-way ANOVA showed no significant difference between the relative rate of [^{3}H]-L-DOPA uptake in the presence of FDOPA, 6-FMT, or L-DOPA. The relative rate of [^{3}H]-L-DOPA uptake was significantly different between the two brain regions for FDOPA ($P < 0.02$) and 6-FMT ($P < 0.03$).

respectively. Similarly, a reduction in [^{3}H]-L-DOPA uptake was also observed in the presence of increasing concentrations of FMT, where the relative rate of [^{3}H]-L-DOPA uptake declined by a maximum of 58 and 44% in synaptosomes isolated from the striatum and cerebral cortex, respectively. The relative rate of [^{3}H]-L-DOPA transport between the two regions investigated was significantly different for FDOPA ($P < 0.02$) and 6-FMT ($P < 0.03$) at all concentrations measured, where the inhibition of [^{3}H]-L-DOPA transport was greater in the striatum compared with the cerebral cortex (Fig. 1). These results are similar to those observed with L-DOPA (unpublished observation).

4. Discussion

4.1. BBB transport

The carotid injection method of Oldendorf [26] was chosen to characterize the transport of FDOPA across the BBB. This is a simple method that directly quantitates the uptake of any compound of interest, and has been used to characterize carrier-mediated transport systems at the BBB. For example, Oldendorf has demonstrated the saturability of substrates, such as biogenic amines, hexoses, and amino acids [27], as well as, the stereospecificity of transport carriers for L-enantiomers of amino acids [28]. The method is based on the direct rapid arterial injection of the radiolabeled probe with the collection of brain tissue 15 sec later. This approach circumvents problems involved with systemic administration of radiolabeled test substances by intraperitoneal or intravenous injection [27].

We showed in this work that [^{18}F]FDOPA, like L-DOPA, does not cross the BBB by way of the alanine-preferred (A-system) LNAA transport mechanism (Table 1), as demonstrated by the inability of the synthetic amino acid MeAIB (a model substrate for the A-system transport mechanism in Ehrlich cells [17]) to decrease [^{18}F]FDOPA brain transport. At a concentration of 2 mM, MeAIB should occupy a majority of the alanine-preferred LNAA carriers to limit severely any contribution from this transport system across the barrier, since the half-maximal transport velocity constant (k_t) for L-DOPA was found to be 336 μM [29]. Instead, L-phenylalanine and L-DOPA competed well against [^{18}F]FDOPA. This suggests that [^{18}F]FDOPA transport across the BBB most likely utilizes the same carrier as these substrates, the L-system LNAA transporter. The comparable BUI of [^{18}F]FDOPA and 3-[^{14}C]L-DOPA after carotid artery injection also supports this parallelism between these two compounds.

In this investigation, the BUIs of two radiolabeled forms of L-DOPA (1-[^{14}C]-L-DOPA and 3-[^{14}C]-L-DOPA) were employed to obtain more precise quantitative information on the BBB entry of L-DOPA. Although the Oldendorf method circumvents peripheral metabolism of the injectant, the presence of brain capillary AAAD may confound the interpretation of results obtained when determining levels of L-DOPA entering the brain. Depending upon where the radiolabel is attached, it can efflux out rapidly or remain within the endothelium for a longer time. For example, the ability to distinguish between the decarboxylated and non-decarboxylated forms of L-DOPA after carotid artery injection of 3-[^{14}C]-L-DOPA is difficult, since the measured BUI of 3-[^{14}C]-L-DOPA represents both radioactivity that has entered the brain, and activity that has been trapped within

brain capillaries after AAAD decarboxylation. This provides an explanation as to why the BUI of 3-[^{14}C]-L-DOPA after carbidopa pretreatment remains essentially unchanged (Table 1). By contrast, carotid artery injection of 1-[^{14}C]-L-DOPA produces a BUI that directly measures the BBB transfer of L-DOPA, and can also serve as a direct indicator of capillary AAAD activity, since the radioactivity detected essentially accounts for intact L-DOPA. Upon decarboxylation of 1-[^{14}C]-L-DOPA, carbon dioxide is released along with the radiolabel. As a result, the presence of the decarboxylated product of L-DOPA trapped in the endothelium is not detected. This produces a BUI of 1-[^{14}C]-L-DOPA which is less than the BUI measured for 3-[^{14}C]-L-DOPA, and also demonstrates that a substantial amount of L-DOPA given by carotid artery injection does not cross the BBB. Unlike results observed with 3-[^{14}C]-L-DOPA, the administration of carbidopa can inhibit brain capillary AAAD activity to increase the BUI of 1-[^{14}C]-L-DOPA (Table 1). Previous work demonstrated that the striatal FDOPA uptake rate constant (K_i) estimated with PET increased as a function of carbidopa dose, where the increase in measured striatal activity was related to an increase in arterial plasma FDOPA concentration [23]. Results presented in this work provides *in vitro* evidence to supports this conclusion.

Previous work demonstrated that hydrazines such as carbidopa can exert their inhibitory effects by either (a) binding tightly to AAAD [30], (b) binding directly to pyridoxal kinase to prevent production of PLP [31], or (c) binding directly to PLP [32]. Indeed, it is unlikely that carbidopa binds to brain endothelium AAAD, an intracellular cytosolic enzyme [33], because it has been shown that carbidopa neither enters nor accumulates in brain tissue [34–36] or brain endothelium [37]. Moreover, the observation that the BUI of 1-[^{14}C]-L-DOPA remained unchanged in the presence of 0.3 or 3.0 μg/mL of carbidopa also suggests the inaccessibility of endothethial AAAD to carbidopa (Table 1). It is also unlikely that carbidopa exerts its effects by binding directly to pyridoxal kinase, since pyridoxal kinase, like AAAD, is not accessible to carbidopa [38]. The most plausible mode of inhibition is a decline in capillary endothelium PLP induced by direct binding of the hydrazine to this cofactor in peripheral tissues. Indirect evidence from this work suggests this, since coinjection of the tracers with pyridoxine appears to reverse carbidopa inhibition in brain capillaries (Table 1). Furthermore, Airoldi and co-workers [39] also found that concurrent administration of pyridoxine can block a carbidopa-induced fall of PLP in tissues. Equally interesting, it appears that carbidopa action is not due to direct interference of carbidopa with BBB transporters, since simultaneous injection of carbidopa (0.3 or 3.0 μg/mL) with 1-[^{14}C]-L-DOPA or 3-[^{14}C]-L-DOPA did not change the BUI of either tracer. This is consistent with data obtained with PET, which showed that carbidopa pretreatment did not affect the BBB transport of [^{18}F]FDOPA, as represented by the influx rate constant K_1 in humans [40]. The consistency observed between the influx rate constant K_1 estimated from PET and that based on the carotid injection method also strengthens the validity of extrapolating [^{18}F]FDOPA transport data from rodent models to interpretations of PET kinetics in primates.

4.2. Neuronal membrane transport

Previous investigations indicate the presence of a substrate transporter for L-DOPA on the neural plasma membrane of striatal synaptosomes [18]. This carrier was found to possess characteristics similar to the LNAA transporter located on the BBB, in that it belongs to the class of transporters known as system-L with specificity for branched chain and aromatic large neutral amino acids [41]. Indeed, we were able to demonstrate that transport across the striatal nerve membrane was due to the presence of a high-affinity carrier, distinctly different from the carrier for L-DOPA found on cortical synaptosomes (unpublished observation). These results have indicated that transport is a contributing factor in determining the preferential accumulation of L-DOPA within the brain. The high cerebral preference of L-DOPA for striatal tissue is also supported by autoradiographic and biochemical evidence in rats [29,42, 43]. Like L-DOPA, intravenous administration of [^{18}F]FDOPA also results in the specific accumulation of F-18 primarily in the basal ganglia [1,2], as demonstrated by PET imaging. These results imply that neuronal plasma transfer of [^{18}F]FDOPA paralleled that of L-DOPA.

To verify this possibility, the regional specificity of [^{18}F]FDOPA accumulation in striatal nerve terminals was examined indirectly by looking at the ability of FDOPA to inhibit the neuronal transport of [^{3}H]-L-DOPA. Previous results demonstrated that in the presence of unlabeled L-DOPA, [^{3}H]-L-DOPA transport in both striatal and cortical synaptosomes was inhibited (unpublished result). The specificity of L-DOPA for striatal terminals was indicated by the greater degree of inhibition observed in terminals isolated from the striatum compared with those of the cerebral cortex. Our observations in this work resulted in similar findings when the inhibition of [^{3}H]-L-DOPA was examined in the presence of FDOPA (Fig. 1). A comparison of the regional inhibition by L-DOPA and FDOPA showed that both compounds were able to compete with [^{3}H]-L-DOPA transport similarly in both striatal and cortical terminals. This consistency suggests that transport of FDOPA parallels that of L-DOPA at the neuronal membrane.

The brain regional transport of other presynaptic dopaminergic probes was also found to be specific for striatal nerve terminals. In this work, 6-FMT was found to be an effective inhibitor of [^{3}H]-L-DOPA transport in the striatum, but was less effective in blocking the uptake of [^{3}H]-L-DOPA in cortical nerve terminals. This is consistent with the observation that tyrosine and other LNAAs are also more effective inhibitors in the striatum, while large neutral aliphatic amino acids were found to be better competitors for L-DOPA transport in the cerebral cortex (unpublished

results). Overall, these observations suggest that neuronal transport of L-DOPA, FDOPA, and 6-FMT compete for similar transport sites.

Transport of amino acids can be described quantitatively by a facilitated transport model that includes a saturable and a non-saturable component [44]. Similar to findings for L-DOPA (unpublished results), the neuronal transport of FDOPA and 6-FMT can also be described by this two-carrier model, in which one carrier shows high-affinity uptake and the other (low-affinity) may be diffusional. The presence of both high- and low-affinity uptake systems would ensure the transport of L-DOPA and its analogs at a wide range of extracellular concentrations. Alterations in transport kinetics can result in severe disturbance in the distribution and relative concentrations of these compounds within the brain. Therefore, understanding BBB and neuronal transport mechanisms is important for evaluation of [^{18}F]FDOPA kinetics with PET and in the therapeutic use of L-DOPA for the treatment of PD.

The derivation of kinetic rate constants to quantitate data obtained from [^{18}F]FDOPA-PET images is possible through the use of compartmental modeling. However, the relevance of this model is dependent upon its accuracy to describe the biological system being examined. Tracer kinetic modeling of [^{18}F]FDOPA has generally been represented in the striatum by a three-compartment model [40]. The rate constants K_1 and k_2 describe the movement of [^{18}F]FDOPA across the BBB, while its subsequent conversion by neuronal AAAD is denoted by k_3. Interestingly, the membrane transport of [^{18}F]FDOPA has not been described in most compartmental models even though it is obvious that [^{18}F]FDOPA must cross cellular membranes for accessibility to neuronal AAAD. However, in the case of central dopamine synthesis from exogenous L-DOPA, transport may be rate-limiting. Previous work demonstrated that neuronal membrane transport of L-DOPA across striatal nerve terminals can decrease the decarboxylation rate of L-DOPA by AAAD at least 5-fold [18]. Kinetic analysis revealed that the L-DOPA K_m of AAAD (100 μM) [45] exceeds that of neuronal transport in the striatum ($K_m = 0.5$ μM) (unpublished observation), providing additional evidence that substrate transport may be limiting.

Like L-DOPA, the metabolic conversion of [^{18}F]FDOPA by neuronal AAAD may also be controlled by its membrane transport. For example, a quantitative comparison of *in vivo* (k_3) to *in vitro* rates in the same set of animals demonstrated that *in vitro* rates were at least 10-fold larger than the *in vivo* "decarboxylation" rates in rodents [46] and primates [9]. Evidence from this work alludes to the possibility of restrictions to limit [^{18}F]FDOPA access to interneuronal AAAD by membrane transport. Just as the LNAA transporter has been implicated in the transport of [^{18}F]FDOPA across the BBB, we have presented evidence in this work of a neuronal membrane transporter involved in carrying [^{18}F]FDOPA into striatal neurons. As a result, [^{18}F]FDOPA tracer kinetics in the striatum may be represented more appropriately by a four-compartment model with neuronal transport as a separate component.

In summary, the experimental data on BBB transfer of [^{18}F]FDOPA suggests that [^{18}F]FDOPA, L-DOPA, and L-phenylalanine share a common LNAA carrier at the BBB in rat brain. This work also demonstrates that plasma carbidopa does not interfere directly with the amino acid carrier at the BBB. Instead, carbidopa inhibition appears to be the result of the depletion of the enzyme cofactor PLP. Similarly, the neuronal transport of FDOPA and 6-FMT parallels that of L-DOPA within the different brain regions. The specificity of the neuronal membrane transport of FDOPA and 6-FMT supports the importance of transport in the regulation of the movement of L-DOPA within the brain. In addition, the evidence presented in this work infers that the rate constant k_3 may actually be composed of a neuronal transport component (k_n) as well as a decarboxylase component (k_{dc}). Thus, implications of a neuronal transporter may affect the interpretation of [^{18}F]FDOPA-PET data.

Acknowledgments

This work was supported by NIH (NS33356) and Department of Energy (DE-FC03-87ER60615) grants.

References

[1] Garnett ES, Firnau G, Nahmias C, Chirakal R. Striatal dopamine metabolism in living monkeys examined by positron emission tomography. Brain Res 1983;280:169–71.
[2] Garnett ES, Firnau G, Nahmias C. Dopamine visualized in the basal ganglia of living man. Nature 1983;305:137–8.
[3] Melega WP, Perlmutter MM, Luxen A, Nissenson CHK, Grafton ST, Huang S-C, Phelps ME, Barrio JR. 4-[^{18}F]Fluoro-L-*m*-tyrosine: an L-3,4-dihydroxyphenylalanine analog for probing presynaptic dopaminergic function with positron emission tomography. J Neurochem 1989;53:311–4.
[4] Barrio JR, Huang S-C, Yu D-C, Melega WP, Quintana J, Cherry SR, Jacobson A, Namavari M, Satyamurthy N, Phelps ME. Radiofluorinated L-*m*-tyrosines: new in-vivo probes for central dopamine biochemistry. J Cereb Blood Flow Metab 1996;16:667–78.
[5] Fowler JS, Volkow ND, Wolf AP, Dewey SL, Schlyer DJ, Macgregor RR, Hitzemann R, Logan J, Bendriem B, Gatley SJ, Christman D. Mapping cocaine binding sites in human and baboon brain *in vivo*. Synapse 1989;4:371–7.
[6] Kilbourn MR, DaSilva JN, Frey KA, Koeppe RA, Kuhl DE. In vivo imaging of vesicular monoamine transporters in human brain using [^{11}C]tetrabenazine and positron emission tomography. J Neurochem 1993;60:2315–8.
[7] Doudet DJ, Miyake H, Finn RT, McLellan CA, Aigner TG, Wan RQ, Adams HR, Cohen RM. 6-^{18}F-L-DOPA imaging of the dopamine neostriatal system in normal and clinically normal MPTP-treated rhesus monkeys. Exp Brain Res 1989;78:69–80.
[8] Leenders KL, Salmon EP, Tyrrell P, Perani D, Brooks DJ, Sager H, Jones T, Marsden CD, Frackowiak RSJ. The nigrostriatal dopaminergic system assessed in vivo by positron emission tomography in healthy volunteer subjects and patients with Parkinson's disease. Arch Neurol 1990;47:1290–8.
[9] Yee RE, Huang S-C, Stout DB, Irwin I, Shoghi-Jadid K, Togaski DM, DeLanney LE, Langston JW, Satyamurthy N, Farahani KF,

Phelps ME, Barrio JR. Nigrostriatal reduction of aromatic L-amino acid decarboxylase activity in MPTP-treated squirrel monkeys: in vivo and in vitro investigations. J Neurochem 2000;74:1147–57.
[10] Huang S-C, Phelps ME. Principles of tracer kinetic modeling in positron emission tomography and autoradiography. In: Phelps ME, Mazziotta JC, Schelbert H, editors. Positron emission tomography and autoradiography: principles and applications for the brain and heart. New York: Raven Press, 1986. p. 287–346.
[11] Barrio JR, Huang S-C, Melega WP, Yu D-C, Hoffman JM, Schneider JS, Satyamurthy N, Mazziotta JC, Phelps ME. 6-[^{18}F]Fluoro-L-DOPA probes dopamine turnover rates in central dopaminergic structures. J Neurosci Res 1990;27:487–93.
[12] Cumming P, Häusser M, Martin WRW, Grierson J, Adam MJ, Ruth TJ, McGeer EG. Kinetics of *in vitro* decarboxylation and the *in vivo* metabolism of 2-^{18}F- and 6-^{18}F-fluorodopa in the hooded rat. Biochem Pharmacol 1988;37:247–50.
[13] Melega WP, Luxen A, Perlmutter MM, Nissenson CHK, Phelps ME, Barrio JR. Comparative *in vivo* metabolism of 6-[^{18}F]fluoro-L-DOPA and [^{3}H]L-DOPA in rats. Biochem Pharmacol 1990;39:1853–60.
[14] Ackermann R, Melega WP, Phelps ME. Selective loss of 3-[^{14}C]-L-DOPA labeling in forebrain mesolimbic structures of rat induced by self-stimulation of dopaminergic neurons in ventral segment area and substantia nigra. J Cereb Blood Flow Metab 1991;11:S608.
[15] Melega WP, Barrio JR, Phelps ME, Ackermann RF. Electrical self-stimulation of rat medial forebrain bundle increases both endogenous dopamine and pulse labeled [^{3}H]L-DOPA striatal metabolism. Soc Neurosci Abstr 1991;17:501.
[16] Rossetti Z, Krajnc D, Neff NH, Hadjiconstantinou M. Modulation of retinal aromatic L-amino acid decarboxylase via α_2-adrenoreceptors. J Neurochem 1989;52:647–52.
[17] Wade LA, Katzman R. Synthetic amino acids and the nature of L-DOPA transport at the blood-brain barrier. J Neurochem 1975;25:837–42.
[18] Katz IR. Inhibition of 3,4-dihydroxy-L-phenylalanine decarboxylase in rat striatal synaptosomes by amino acids interacting with substrate transport. Biochim Biophys Acta 1980;600:195–204.
[19] Bertler A, Falck B, Rosengren E. The direct demonstration of a barrier mechanism in the brain capillaries. Acta Pharmacol Toxicol (Copenh) 1963;20:317–21.
[20] Hardebo JE, Falck B, Owman C, Rosengren E. Studies on the enzymatic blood-brain barrier: quantitative measurements of DOPA decarboxylase in the wall of microvessels as related to the parenchyma in various CNS regions. Acta Physiol Scand 1979;105:453–60.
[21] Marsden CD, Parkes JD, Rees JE. A year's comparison of treatment of patients with parkinson's disease with levodopa combined with carbidopa versus treatment with levodopa alone. Lancet 1973;2:1459–62.
[22] Chan GL-Y, Doudet DJ, Dobko T, Hewitt KA, Schofield P, Pate BD, Ruth TJ. Routes of administration and effect of carbidopa pretreatment on 6-[^{18}F]fluoro-L-DOPA/PET scans in non-human primates. Life Sci 1995;56:1759–66.
[23] Hoffman JM, Melega WP, Hawk TC, Grafton SC, Luxen A, Mahoney DK, Barrio JR, Huang S-C, Mazziotta JC, Phelps ME. The effects of carbidopa administration on 6-[^{18}F]fluoro-L-DOPA kinetics in positron emission tomography. J Nucl Med 1992;33:1472–7.
[24] Luxen A, Perlmutter M, Bida GT, Van Moffaert G, Cook JS, Satyamurthy N, Phelps ME, Barrio JR. Remote, semiautomated production of 6-[^{18}F]fluoro-L-dopa for human studies with PET. Appl Radiat Isot 1990;41:275–81.
[25] Namavari M, Satyamurthy N, Phelps ME, Barrio JR. Synthesis of 6-[^{18}F] and 4-[^{18}F]fluoro-L-*m*-tyrosines via regioselective radiofluorodestannylation. Appl Radiat Isot 1993;44:527–36.
[26] Oldendorf WH. Measurement of brain uptake of radiolabeled substances using a tritiated water internal standard. Brain Res 1970;24:372–6.
[27] Oldendorf WH. Brain uptake of radiolabeled amino acids, amines, and hexoses after arterial injection. Am J Physiol 1971;221:1629–39.
[28] Oldendorf WH. Stereospecificity of blood-brain barrier permeability to amino acids. Am J Physiol 1973;224:967–9.
[29] Wade LA, Katzman R. Rat brain regional uptake and decarboxylation of L-DOPA following carotid injection. Am J Physiol 1975;228:352–9.
[30] Jung MJ. Substrates and inhibitors of aromatic amino acid decarboxylase. Bioorg Chem 1986;14:429–43.
[31] McCormick DB, Snell EE. Pyridoxal kinase of human brain and its inhibition by hydrazine derivatives. Proc Natl Acad Sci USA 1959;39:1371–9.
[32] Clark WG. Studies on inhibition of L-DOPA decarboxylase *in vitro* and *in vivo*. Pharmacol Rev 1959;11:330–49.
[33] Bowsher RR, Henry DP. Aromatic-L-amino acid decarboxylase: biochemistry and functional significance. In: Boulton AA, Baker GB, Yu PH, editors. Neuromethods, Series 1: neurochemistry, neurotransmitter enzymes. New Jersey: Humana Press, 1986. p. 33–77.
[34] Lotti VJ, Porter CC. Potentiation and inhibition of some central actions of L(−)-dopa by decarboxylase inhibitors. J Pharmacol Exp Ther 1970;172:406–15.
[35] Porter CC, Watson LS, Titus DC, Totaro JA, Byer SS. Inhibition of dopa decarboxylase by the hydrazino analog of α-methyldopa. Biochem Pharmacol 1962;11:1067–77.
[36] Vickers S, Stuart EK, Bianchine JR, Hucker HB, Jaffe ME, Rhodes RE, Vandenheuvel WJA. Metabolism of carbidopa [L-(−)-α-hydrazino-3,4-dihydroxy-α-methylhydrocinnamic acid monohydrate], an aromatic amino acid decarboxylase inhibitor, in the rat, dog, rhesus monkey, and man. Drug Metab Dispos 1974;2:9–22.
[37] Clark WG, Oldendorf WH, Dewhurst WG. Blood-brain barrier to carbidopa (MK-486) and Ro 4-4602, peripheral dopa decarboxylase inhibitors. J Pharm Pharmacol 1973;25:416–8.
[38] Wada H, Morisue T, Sakamoto Y, Ichihara K. Quantitative determination of pyridoxal phosphate by apotryphanase of *Escherichia coli*. J Vitaminol (Kyoto) 1957;3:183–8.
[39] Airoldi L, Watkins CJ, Wiggins JF, Wurtman RJ. Effect of pyridoxine on the depletion of tissue pyridoxal phosphate by carbidopa. Metabolism 1978;27:771–9.
[40] Huang S-C, Yu D-C, Barrio JR, Grafton S, Melega WP, Hoffman JM, Satyamurthy N, Mazziotta JC, Phelps ME. Kinetics and modeling of L-6-[^{18}F]fluoro DOPA in human positron emission tomographic studies. J Cereb Blood Flow Metab 1991;11:898–913.
[41] Christensen HN, Liang M, Archer EG. A distinct Na^+-requiring transport system for alanine, serine, cysteine, and similar amino acids. J Biol Chem 1967;240:5237–46.
[42] Glowinski J, Iversen LL. Regional studies of catecholamines in the rat brain-I. The disposition of [^{3}H]norepinephrine, [^{3}H]dopamine and [^{3}H]DOPA in various regions of the brain. J Neurochem 1966;13:655–69.
[43] Horne MK, Cheng CH, Wooten GF. The cerebral metabolism of *L*-dihydroxyphenylalanine. An autoradiographic and biochemical study. Pharmacology 1984;28:12–26.
[44] Daniel PM, Pratt OE, Wilson PA. The transport of L-leucine into the brain of the rat *in vivo*: saturable and non-saturable components of influx. Proc R Soc Lond B Biol Sci 1977;196:333–46.
[45] Reith J, Dyve S, Kuwabara H, Guttman M, Diksic M, Gjedde A. Blood-brain transfer and metabolism of 6-[^{18}F]fluoro-L-DOPA in rat. J Cereb Blood Flow Metab 1990;10:707–19.
[46] Cumming P, Kuwabara H, Gjedde A. A kinetic analysis of 6-[^{18}F]fluoro-L-dihydroxyphenylalanine metabolism in the rat. J Neurochem 1994;63:1675–82.